

STRUCTURAL DESIGN STUDIES OF A
SUPERSONIC CRUISE ARROW WING CONFIGURATION

Jaroslav Sobieszczanski
NASA Langley Research Center

and

L. Arnold McCullers, Rodney H. Ricketts, Nick J. Santoro,
Sharon D. Beskenis, and William L. Kurtze
Vought Corporation Hampton Technical Center

SUMMARY

Structural member cross sections were sized with a system of integrated computer programs to satisfy strength and flutter design requirements for several variants of the arrow wing supersonic cruise vehicle. The resulting structural weights provide a measure of the structural efficiency of the plan-form geometry, structural layout, type of construction, and type of material including composites.

A study was conducted to determine the material distribution for a baseline metallic structure. The results of this study indicated that an approximate fatigue constraint has an important effect on the structural weight required for strength but, in all cases, additional material had to be added to satisfy flutter requirements. It also proved to be more difficult to satisfy flutter requirements with lighter mass engines with minimum fuel onboard.

A study was performed on a reduced wing area configuration which indicated that although the wing loading was higher than the baseline, the structural mass required to satisfy strength and flutter requirements decreased.

The use of composite materials on the baseline configuration was explored and indicated increased structural efficiency. In the strength sizing, the all-composite construction provided a lower weight design than the hybrid construction which contained composites only in the wing cover skins. Subsequent flutter analyses indicated a corresponding lower flutter speed.

INTRODUCTION

The reported studies are part of the current Langley Supersonic Cruise Aircraft Research (SCAR) program. One of the primary goals of this program is to investigate the design technology for minimum weight supersonic aircraft, strength and flutter requirements for metallic and composite primary structure being considered. The arrow wing configuration, shown in figure 1, in a subsonic

leading-edge wing optimized for low drag due to lift at supersonic speeds. The uniqueness of this planform precludes the use of only statistical data for a reliable estimate of the primary structural mass. Therefore, structural mass estimates have to be supplied by analytical studies such as reported in this paper. Inputs to this work, such as geometric shape, weight breakdown, and material data, were provided by other in-house studies and contractor studies.

This paper devotes separate sections to the development of the baseline configuration, the effect of reducing the wing area, and the influence of composite materials.

An associated goal of the SCAR program involves the development and integration of the computerized tools needed for aircraft structural design. An abbreviated discussion of the tools used to generate the results presented in this paper is given in the appendix.

BASELINE CONFIGURATION (AST 9)

A study was conducted to determine the material distribution for the baseline configuration meeting strength and flutter criteria and utilizing titanium construction. This structural baseline was developed by exploring a number of variants and is used as a basis of comparison for subsequent designs. The study method, the analytical model, and the results of this study are discussed in the following subsections.

Analytical Approach

In general, the exploration of a variant of the configuration consists of the following operations:

(1) Static structural analysis is performed by using a finite-element method accounting for the aeroelastic loads and the jig shape. Trimming the aircraft at each design flight condition is included in the static structural analysis.

(2) Cross sections of selected structural components, usually the wing cover panel skins and the rib and spar shear webs, are sized to satisfy the static strength requirements with minimum structural mass. The techniques used here are the weight-strength method for metal construction, and the more general mathematical nonlinear programming method whenever composite material is involved. Operations (1) and (2) are collectively referred to as the strength design.

(3) Flutter analysis is performed on this strength design in the complete operational velocity-altitude envelope.

(4) The cross sections are resized for greater overall stiffness and minimum additional structural mass (flutter penalty) to eliminate any flutter deficiency.

The methodology involved in these operations and the computer implementation are outlined in the appendix.

All four operations are not always necessary to evaluate the variant under study. Operation (4), the most costly, is frequently omitted if the first three operations do not indicate a major advantage for that variant.

Structural mass is adopted as an ultimate figure of merit to judge the configuration studied, except in the cases when operation (4) is not carried out. In such cases, both structural mass and flutter speed deficiency are used to judge the potential structural efficiency.

Baseline Analytical Model

The basic information for the baseline configuration, shown in the table on figure 1, includes the take-off gross weight (TOGW), operational empty weight (OEW), and payload (PL) which serve as references for quoting the structural weight results. The finite-element model representation of this configuration and the type of construction are shown in figure 2. The wing is built up of corrugated web spars and ribs with caps supporting honeycomb sandwich covers. Conventional stringer-skin-frame construction is used in the fuselage.

Finite-element model. In the finite-element model, the covers are simulated by membrane elements, spar and rib webs by shear panels, and caps by rod elements. Beam elements are used to represent the engines, the engine mounts, and the supports for leading- and trailing-edge devices. Plate elements are used to model the vertical fins and horizontal stabilizers. Nonstructural components are represented by appropriate lumped and distributed masses. For computation economy, the fuselage model is simplified to a rectangular cross-section box with overall bending stiffness and mass equivalent to the fuselage. This simplification is consistent with the study's emphasis on the primary wing structure; as a result the rest of the airframe is excluded from the resizing process, but not from the analysis. The construction material is titanium throughout the primary structure. The resulting half airplane finite-element model has 746 grid points, 2141 degrees of freedom, and 2369 finite elements.

Material properties and allowables. The titanium data used in this study are displayed in the first row of table 1. The allowable stress level for cruise is restricted to the value designated FAC (for Fatigue Allowable Cruise) in order to approximately account for fatigue requirements. In titanium construction, this value corresponds to a notch factor of 4.0. The data for the honeycomb core and core-face sheet bonding are also included in table 1.

Loading cases. From the multitude of loading cases considered in the design of airframes, the three cases shown in table 2, together with their limit load factors, were selected for use in the strength sizing. These three cases are judged to be sufficiently representative for the purpose of this study. The cruise case defines the jig shape and accounts approximately for fatigue,

the maneuver case generates the largest wing root bending moment, and the taxi loads expose the wing lower surface covers to compression. A safety factor of 1.5 is used to define the ultimate (design) load factors.

Four fuel conditions are used in the analyses: (1) full fuel for taxi (TF), (2) heavy fuel (HF) at the maneuver design point during climb, (3) cruise fuel (CF) at the start of cruise, and (4) light fuel (LF) at the maneuver design point during descent. The appropriate fuel inertia forces are included in the design loads for each load condition.

Baseline Results

A number of strength designs, flutter analyses, and flutter designs were performed on the baseline configuration. The results are discussed in the subsequent sections.

Strength design results. A total of 334 wing cover panels and 384 shear webs are subject to sizing in this operation. The spar and rib cap areas and other parts of the airframe are held constant. In the cover panels, the sandwich depth is also kept constant, 2.54 cm (1 in.), so that the face sheet thicknesses are the only variables. A contour map of the resulting skin thickness distribution is shown in figure 3. It shows characteristic islands of thickness which reflect the local stress concentrations in the vicinity of the vertical fin (A), the rear spar crank (B), and the wheel well (C). These concentrations are also evident in the contour map of the upper surface principal stress distribution for the maneuver case, illustrated in figure 4.

Distribution of the critical loading conditions over the upper cover of the wing is shown in figure 5. The outboard part of the wing is dominated by the cruise-fatigue requirements, whereas the maneuver condition is critical for the inboard aft part of the wing box. The influence of the taxi condition is limited to the vicinity of the wheel well. Large areas of the wing have minimum gage thickness covers.

The mass of the strength design is 27 266 kg (60 120 lbm) for the wing structure of the airplane. This includes load-carrying material comprised of the sandwich cover's face sheets, rib and spar caps, and shear webs, and additional mass due to corrugations in the shear webs, core, and bonding.

In order to account for the mass of joints, fasteners, padding, and so forth, an incremental nonoptimum factor is applied to the mass of load-carrying material. To conform to the statistical weight data available as input to these studies, a factor of 0.3125 is present in all mass results reported, unless indicated otherwise.

Results of auxiliary analyses. The strength design was analyzed for thermal stress, extended flap loads, and reduced fuel mass inertia relief in order to check for critical conditions not included in the basic loading cases. The results were as follows:

(1) Thermal analysis revealed that the thermal stress increments in the wing cover panels are relatively small in comparison with the maneuver loading

case stress. The largest thermal stresses are 9 to 10 percent of the maneuver stresses in about 5 percent of the panels.

(2) The extended flap analysis was conducted for a load factor of 1.65 (landing with gust) with flap deflections varying from 24° inboard to 5° at the wing tip. This indicated no overstressed elements.

(3) Analysis with the lightweight fuel showed no overstressed elements and confirmed the criticality of the heavy weight fuel maneuver condition for the strength design.

Flutter analysis. Symmetric flutter analyses of the strength designed wing showed that the structure did not meet the flutter speed requirement of 1.2 V_D (dive velocity) for various combinations of fuel loadings and engine weights. In figure 6, a typical set of results for the original 10 431 kg (23 000 lbm) engines (designated E23) shows that the structure is more deficient in the subsonic region than in the supersonic region and has three distinct flutter modes that can be critical. Also, the analyses showed that the lightweight fuel condition with alternate 7 483 kg (16 500 lbm) engines (designated E16) provided the worst combination for flutter fixing.

Results of the flutter fix. Subsequent to the strength design, a flutter fix was carried out by means of a trial-and-error procedure (outlined in the appendix) for the E23 baseline engine. The additional thicknesses of the wing covers needed to meet the flutter requirements were combined with the strength designed thicknesses by means of a "minimum gage technique" described in the appendix. Combining the two sets of thicknesses has a smoothing effect on the distribution as illustrated by figure 7. The three flutter modes which were critical during the flutter analysis of the strength-sized structure were removed beyond the required envelope as shown in figure 8. A "hump" flutter mode which appeared and disappeared during the flutter fix operation made the flutter resizing more difficult. The final wing design has a total structural mass of 28 810 kg (63 524 lbm). The mass increment (flutter penalty) of 1 544 kg (3 404 lbm) comes entirely from the increased cover thickness and represents a 5.7-percent increase in the structural mass.

A similar flutter fix for the alternate engine (E16) produced a structural mass increase to a total of 30 166 kg (66 514 lbm), a flutter penalty of 2 900 kg (6 394 lbm). Comparison of the structural masses for the cases with engines E23 and E16 shows that the decrease in engine mass more than offsets the structural mass increase (10.6 percent) due to flutter penalty for a net mass decrease of 10 436 kg (23 010 lbm). Because of the lower overall mass and the increased difficulty in flutter sizing, the alternate engine case (E16) was selected for subsequent flutter analyses.

Antisymmetric flutter analysis. The flutter fixed design was analyzed for flutter by using antisymmetric vibration modes and airloads. The results showed that the structure was slightly deficient in flutter speed (0 to 3.3 percent) in the subsonic region. This deficiency was judged to be too small to justify another flutter fix resizing cycle. However, it demonstrated that the antisymmetric flutter modes must be checked for this type of vehicle.

Influence of aeroelastic loads and fatigue allowable. Three additional strength designs were performed to explore the impact of aeroelastic effects in the maneuver load condition and the effect of the cruise-fatigue condition on structural mass. In the first additional design, the baseline configuration was resized with rigid maneuver loads, that is, the maneuver load vector was not updated to include aeroelastic effects. Because of the lack of aeroelastic load relief, this resulted in a structural weight increase of 12.8 percent with almost the entire wing designed by the maneuver condition.

The second and third designs were used to study the effect of the fatigue allowable. The second was performed with flexible maneuver loads and a 33-percent increase in the fatigue allowable. The structural weight dropped 4.5 percent with very few structural elements designed by the cruise-fatigue condition. In the third design, removing the cruise-fatigue condition entirely resulted in only an additional 0.1 percent (total 4.6 percent) structural weight decrease.

Influence of modified carry-through design. The baseline configuration has only the spar caps, typical of floor beams, continuous across the fuselage ahead of the wheel wells. To study the design impact of these moment carrying members, the wing structure was redesigned with these spar caps deleted.

This variant is of interest for two reasons. First, it allows the wing root chord and the fuselage to be longitudinally shaped independent of each other. Thus, the wing root camber may be designed solely by aerodynamic considerations, and the fuselage may be designed by both aerodynamic and passenger comfort considerations. (The fuselage is not forced to assume a form with excessive passenger floor slopes due to cruise angle of attack.) Secondly, it opens the possibility to design the wing-fuselage intersection along the section marked 1 in figure 9 so that the wing's highest temperature area will have the freedom to expand thermally and thus reduce the thermal stress. Strength design of the airframe modified in this manner resulted in a structural mass increase of 1.7 percent over the baseline strength sized configuration.

Subsequent flutter analysis of this design revealed that there is a change in the flutter modes and frequencies but no appreciable change in the lowest flutter speed. It was concluded that the variant is structurally viable and may be adopted in the vehicle design if desired.

Influence of structural box planform geometry. In order to relieve the stress concentration shown in figure 4 in the vicinity of the rear spar crank, the modified planform shown in the figure 9 inset with a "double crank" was strength sized. Even though there was some stress relief in the area of the crank, there was a negligible difference in the structural mass that indicated further study of this variant was not warranted.

Selection of structural baseline. Based on the results discussed in the preceding paragraphs, the material distribution generated by strength sizing the baseline configuration with the E23 engines and the heavy weight maneuver (HF) fuel was selected as the strength sized baseline for comparison with other configurations. The mass and material distribution resulting from

the flutter fix with the lightweight maneuver (LF) fuel and the alternate E16 engines was used for flutter design comparison since this is a more severe case from a flutter standpoint.

REDUCED WING AREA CONFIGURATION (AST 10)

A configuration with a smaller wing was studied because of its improved aerodynamic performance. It is geometrically similar to the baseline with a 15.3-percent reduction in wing area and no change in the fuselage. The relative position of the wing on the fuselage is changed, however, because of aircraft balance requirements. Propulsion system requirements for this variant call for an engine weight of 6 647 kg (14 656 lbm), designated E14. The configurations TOGW and OEW are reduced to 325 624 kg (718 000 lbm) and 139 507 kg (307 612 lbm), respectively, with the payload unchanged. A strength design, a flutter analysis, and a flutter fix were executed for this configuration in a manner similar to that used in the baseline configuration study. Comparison of the results with those given in the subsection "Results of the Flutter Fix" for the baseline configuration shows a strength design structural mass decrease of 10.5 percent (this is less than the area reduction because of higher wing loading) and a flutter penalty decrease of 35.5 percent. This results in a total primary structural mass decrease of 12.9 percent for AST 10.

COMPOSITE MATERIALS CONFIGURATION (AST 11)

The composite material effect on the primary structural mass has been studied by examining a configuration identical with the baseline (AST 9) with composite primary structure. The composite design problem is more difficult since with composite materials each mechanical property can assume several possible values depending on material selection; there are a number of ways in which the fibers can be laid out; and the degree to which the composite is combined with metal can be varied. A number of variants of the composite configuration have been explored to assess the broad range of the available combinations of these factors.

Material Properties and Allowables

Graphite-polyimide is an attractive composite material for supersonic cruise applications because of its relatively good retention of mechanical properties at elevated temperatures. The material properties, displayed in table 1, were supplied by The Boeing Company. In order to establish upper and lower bounds, the properties anticipated to be commonly available in 1986 are included with those available in 1975. In addition, a pessimistic allowable strain is considered to establish a lower and safer bound on the stress allowables. The fiber volume is assumed to be 60 percent throughout. Note that the composite is available in a low Young's modulus and high strength version and a high Young's modulus and low strength version. In the discussion to follow, use of the low modulus version is assumed unless otherwise indicated. Insofar as the fatigue

stress allowables for cruise are concerned, no data similar to those used for titanium construction exist for composites. However, for consistency, the ratio of the allowable cruise stress to the design limit stress for composites has been set equal to the ratio of the fatigue allowable to the design limit stress for titanium.

Both room temperature, 21° C (70° F), and elevated-temperature, 232° C (450° F), properties are provided for the graphite-polyimide composite in table 1. The differences between the two sets of values are not large; they range from under 10 percent for stress to zero for modulus. Since the 1986 room-temperature data are the most optimistic ones available, they were used unless indicated otherwise for the sake of establishing a consistent upper bound on the results reported.

Hybrid Composite-Titanium Construction (AST 11.1)

In this construction variant, the titanium spars and ribs are retained and the composite is used for the wing covers only. The hybrid construction is of interest as an interim stage between the metal and composite technologies. The composite layup used for strength design is shown in figure 10. It is an orthotropic layup that has the plies oriented at four different filament angles: (0°, + ϕ , 90°) and has the thicknesses in the ϕ -direction set equal (that is, $t_\phi = t_{-\phi}$). In addition to ϕ and t_ϕ , the design variables for this type of construction include the following: thickness, t_o and t_{90} ; depth of the sandwich panel, h ; and the orientation angle of the complete laminate, γ . The design variables are used in a mathematical optimization technique to size the composite sandwich panels as outlined in the appendix. The titanium caps are protected from overstress by strain constraints applied to the composite skins in the optimization procedure.

Hybrid construction baseline. In the basic variant (designated 11.1.1), the three thicknesses, t_o , t_ϕ , and t_{90} , are free design variables. The other variables are frozen as follows: $\phi = 45^\circ$, $\gamma = 0^\circ$, and h is 2.54 cm (1 in.) over most of the wing and 4.45 cm (1.75 in.) where additional depth is required for panel stability.

The results of the strength design, shown as skin-thickness contour maps, are shown in figure 11. The mass of the strength design is 21 825 kg (48 125 lbm), a decrease of 20 percent from the metal baseline strength design. The mass includes previously defined nonoptimum incremental factors. For the titanium parts, a factor of 0.3125, the same as for metal construction, is applied. For the composite parts, a higher value of 0.50 is used in order to compensate conservatively for the smaller pool of weight data available for composite structures. Flutter analysis showed that this variant has a large flutter speed deficiency as illustrated in figure 12. This deficiency is about twice as large as the one for the metallic baseline strength design shown in figure 6.

A subsequent flutter fix, using the "small model and large model" trial-and-error technique explained in the appendix, produced a flutter-free design at the price of a sandwich skin structural mass increment of 4 172 kg (9 200 lbm). The

total structural mass is 25 997 kg (57 325 lbm) which is smaller than the value for the metal, flutter-fixed baseline by 4 169 kg (9 189 lbm) or 14 percent. This is the only composite design to be resized for flutter to date.

Influence of the choice of design variables. Six variants (11.1.2-7) of different groupings of the free and frozen design variables were strength designed and flutter analyzed in addition to the basic variant. The results in terms of the structural mass and flutter speed increments compared with the metal, flutter-fixed baseline are shown in table 3. It is evident that the influence of the choice of the design variables on both structural mass and flutter speed is significant. As expected, the larger the number of free design variables, the lower the structural mass, and the higher the computer cost. From table 3, one can identify case 11.1.5 as the most promising based on the ratio of the mass saved to flutter speed deficiency ($\Delta M/\Delta V$).

Since the sandwich cover panels are optimized individually (see the appendix), the variants with free orientation angles and sandwich depth may be unacceptably difficult and costly to fabricate by using the standard manufacturing methods. Investigation of these variants has been carried out in order to explore potential benefits. If these benefits are large enough, a revision of the fabrication methods may become justified. The fabrication requirements can also be incorporated in the design itself, at the price of some departure from the minimum mass, by averaging the core depth and orientation variables over large areas of the wing.

Influence of using the high modulus composite. As shown in table 1, the high Young's modulus and relatively lower strength graphite-polyimide is an alternative to the low modulus version used to generate these results. Substitution of the alternative properties in the strength design of the basic variant 11.1.1 showed the structural mass to be 8.3 percent larger than that for the low modulus material. However, the flutter analysis indicated less flutter speed deficiency for the high modulus design, as seen in the right half of figure 12, and lift the issue of which version is more efficient to be settled by the flutter fix operation.

Influence of using conservative allowables. Relatively low allowables are sometimes imposed on the fiber strain to produce a conservative design in order to account for many unknown behavior characteristics of composite materials. A strength design of the basic variant (11.1.1), with an ultimate fiber strain limit of 0.006 for the strength constraint, produces a structural mass increase of 7.2 percent. The flutter speed is also higher (73 percent against 63 percent of the required speed) so that the mass cost of using conservative allowables must be provided by the results of the flutter-fix operation.

Pure Composite Construction (AST 11.2)

The relatively high contribution of the titanium caps and webs to the total structural mass of the hybrid construction points to the complete replacement of the titanium by composites as a means to realize potentially large mass savings. The titanium caps not only contribute mass, but also, as mentioned

before, have to be protected from overstress that would prevent the composite from reaching its full load-carrying capacity in many cases.

The pure composite construction consists of composite sandwich cover panels and composite rib and spar shear webs without caps. The only titanium parts retained were the local reinforcements such as engine mounts, and so forth.

The strength design resulted in structural masses of 11 990 kg (26 437 lbm) for the low modulus material and 13 807 kg (30 445 lbm) for the high modulus material, 45.1 percent and 36.7 percent savings, respectively, over the hybrid baseline AST 11.1.1. Flutter analysis results for this construction using low modulus and high modulus material are presented in figure 13. These results show a decrease in flutter speed from AST 11.1.1, 52 percent against 63 percent of the required speed for the low modulus material and 87 percent against 91 percent for the high modulus material.

DISCUSSION OF THE RESULTS

A bar chart comparing the primary variants is shown in figure 14. The wing structural mass from the strength design of the metallic baseline configuration (AST 9) was 17 percent of the operational-empty weight (OEW) and 99 percent of the payload (PL). With the flutter-fix penalty mass added to the strength design mass, the structural mass increased to 19 percent of OEW and 109 percent of PL. Replacing the E23 engines by the E16 engines for this configuration added to the flutter-fix penalty mass but not enough to offset the engine mass savings. This resulted in a decrease of 6.6 percent of OEW and 37.7 percent of PL.

For the reduced wing area configuration (AST 10), the wing structural mass decreased by 2 percent of OEW and 14 percent of PL including the flutter-fix penalty mass.

The change from the metallic baseline configuration (AST 9) to the hybrid configuration (AST 11.1) gave a strength- and flutter-sized structural mass of 16 percent of OEW and 94 percent of PL, a savings of 2 percent of OEW and 10 percent of PL. There is a large decrease in mass due to the strength design, but it is partially offset by a relatively larger flutter-fix penalty mass. Substitution of the high modulus and low strength composite material for the low modulus and high strength composite material gave a strength design structural mass increase of 8 percent of the low-modulus, high-strength design. The use of a more conservative allowable for the low modulus composite material resulted in a strength design structural mass increase of 7 percent compared with the hybrid composite baseline, AST 11.1. Significant structural mass savings for the hybrid configuration were realized by including the sandwich depth as a design variable in the optimization procedure.

To realize fully the mass saving potential of composite materials, an all-composite construction variant (AST 11.2) was explored. The decrease in mass after strength design was 56 and 49 percent of the metallic baseline

configuration for the low and high-modulus composite material, respectively. These are 36 percent larger savings than those of the strength-sized hybrid configurations. Because of the increased flexibility of the all-composite configurations, the flutter-fix penalties would probably be larger than those for the hybrid configurations. Therefore, some of the gain in mass savings would be offset by the increase in the flutter penalty.

CONCLUDING REMARKS

In the main body of the paper, the results were compared on the basis of the total wing structural mass to highlight the large decrease in structural mass when all-composite construction was used (deleting the titanium spar caps). In the discussion of the results, the masses were compared with the operational empty weight and the payload to emphasize the impact on the aircraft. In all studies, the fuselage and control surface masses were held constant. Redesign and/or application of composites to these areas would generate additional weight savings.

Since the wing skins were of primary interest in the resizing, the following observations are based on the mass of the wing skins only.

1. For titanium construction, the arrow wing configurations being studied were made flutter free by increasing the wing skin mass by 15 to 28 percent of the strength-sized skin mass. This increment provides a target mass for the design of an active controls flutter-suppression system.

2. The flutter behavior and the associated mass penalty were significantly affected by the engine mass.

3. Wing-tip washout aeroelastic effects provided load relief savings of about 24 percent of the skin mass for the strength design.

4. Imposition of the fatigue allowable stress on the cruise condition increased the skin mass by 14 percent.

5. Use of composite materials with titanium substructure (webs and caps) saved 55 percent of the skin mass for the strength designs but only 33 percent of the skin mass for the flutter-free designs.

6. The all-composite construction has a much higher mass savings potential as indicated by the strength design results.

7. The use of a high modulus, low strength composite material increased the skin mass by 41 percent for the strength design. This trend may be reversed when a flutter-free design is generated.

8. The methods outlined in the appendix for strength design and flutter analysis proved to be efficient and reliable tools for this application. They also have potential applicability to similar studies of advanced aircraft.

APPENDIX

ANALYSIS AND SYNTHESIS METHODS

The methods used to produce the results reported in this paper are discussed in this appendix. The building blocks of the methodology consist of computer programs for aerodynamic analysis, stress-deflection-vibration analysis, flutter analysis, and data preparation as well as optimization and data handling techniques. Computer graphics are used to display the results. All programs are integrated into a system, as described in reference 1; this integration allows a hands-off data flow among the programs and interactive, as well as batch, executions of sequences of programs.

The study consists of two basic phases: (1) strength analysis and synthesis, and (2) flutter analysis and synthesis.

Strength Analysis and Synthesis

Phase 1 consists of two iterative procedures, one for converging the aeroelastic loads, and the other for resizing the structural cross sections. The two iterations are performed simultaneously as illustrated in figure 15 and described in reference 2. They involve aerodynamic loads computation (ref. 3) stress-deflection analysis, computation of a jig shape, and resizing of the wing individual cover panels and shear webs. Spar and rib caps remain constant in the resizing procedure. The titanium covers are resized by the weight-strength method considering stress, local buckling, and minimum gage (ref. 4). For the composite wing cover panels, the resizing is performed by means of a mathematical programming method applied to each panel separately, as discussed in reference 5, by using the feasible-usable directions technique. Structural mass is the object function in all cases. A comprehensive list of stress, strain, fiber-matrix interaction, local buckling, and geometry constraints for the composite layups are handled by this technique.

Flutter Analysis and Synthesis

The flutter analysis begins with the generation of the vibration mode and frequency data by using the structures finite-element analysis computer program, SPAR. These modes are used to calculate subsonic and supersonic unsteady aerodynamic forces (refs. 6 and 7) which, in turn, are used in the usual k-method flutter analysis. The analysis is entirely automated to produce vibration mode plots, $V-g$ and $V-\omega$ plots, and matched point flutter speeds.

The vibration-flutter analysis sequence has been validated by means of wind-tunnel experiments of an arrow wing aeroelastic model undertaken in support of these studies. Resizing to meet the flutter speed requirements (flutter fix) is performed in a trial-and-error manner based on engineering judgment formed by comparing the flutter boundaries with the required flutter free envelope on the velocity-altitude graph and by inspecting the flutter modes. The selected

stiffening is implemented, and the vibration-flutter analysis is repeated in an iterative manner, characterized in figure 16, until a satisfactory result is obtained.

Three different methods of flutter fix stiffening were evaluated:

(1) scaling the strength designed wing cover thickness, (2) adding patches on top of the strength designed thicknesses, and (3) adding the thickness as a new minimum gage to the strength design. The last method has been found to produce the least flutter-fix penalty and was adopted as a flutter-fix tool.

Flutter Synthesis of the Composite Wing

In the case of composite wing covers, the flutter speed deficiency can be removed not only by means of increasing the overall skin thickness in the manner described above, but also by increasing thicknesses at selected orientations, adding plies of a new orientation, or changing the existing ply orientation angles.

Because of the intrinsically large number of possibilities that need to be explored in order to define a flutter-free composite structure, it is prohibitively expensive to use the same finite-element model which is used in the strength analysis in the trial-and-error loop (fig. 16). Therefore, that model is replaced in the flutter analysis by a different model having the degrees of freedom and finite elements reduced to 387 and 77, respectively. This "small model," shown in figure 17, was made dynamically similar to the large model by means of (1) retaining the overall geometry, (2) using plate elements (representing the full-depth wing) with bending stiffness matrices equivalent to those of the corresponding areas of the large model, (3) defining the fuselage as a stiffness equivalent beam, and (4) retaining the concentrated and distributed masses. Transfer of the stiffnesses (by the cover ply thicknesses and orientation angles) between the two models is fully automated. The flutter-free designs are produced by the same, previously outlined, trial-and-error procedure (fig. 16) by using the small model whose vibration-flutter analysis is more than an order of magnitude less expensive than that for the large model. Final results of each trial-and-error iterative sequence are analyzed for flutter and strength upon transfer to the large model.

REFERENCES

1. Sobieszczanski, Jaroslaw: Building a Computer-Aided Design Capability Using a Standard Time Share Operating System. Proceedings of the ASME Winter Annual Meeting, Integrated Design and Analysis of Aerospace Structures, Houston, Texas, November 30-December 5, 1975, pp. 93-112.
2. Giles, Gary L.; and McCullers, L. A.: Simultaneous Calculation of Aircraft Design Loads and Structural Member Sizes. Presented at the AIAA 1975 Aircraft Systems and Technology Meeting, Los Angeles, California, August 4-7, 1975. (AIAA Paper No. 75-965.)
3. Carmichael, Ralph L.; and Woodward, Frank A.: An Integrated Approach to the Analysis and Design of Wings and Wing-Body Combinations in Supersonic Flow. NASA TN D-3685, 1966.
4. Giles, Gary L.: Procedure for Automating Aircraft Wing Structural Design. Journal of the Structural Division, ASCE, January 1971, pp. 99-113.
5. Sobieszczanski, Jaroslaw: Sizing of Complex Structure by the Integration of Several Different Optimal Design Algorithms. AGARD Lecture Series No. 70 on Structural Optimization, AGARD-LS-70, September 1974.
6. Watkins, Charles E.; Woolston, Donald S.; and Cunningham, Herbert J.: A Systematic Kernel Function Procedure for Determining Aerodynamic Forces on Oscillating or Steady Finite Wings at Supersonic Speeds. NASA TR R-48, 1959.
7. Donato, Vincent W.; and Huhn, Charles R., Jr.: Supersonic Unsteady Aerodynamics for Wings With Trailing Edge Control Surfaces and Folded Tips. AFFDL-TR-68-30, U.S. Air Force, Aug. 1968. (Available from DDC as AD 840598.)

TABLE 1.- MATERIAL PROPERTIES USED IN THE STUDIES

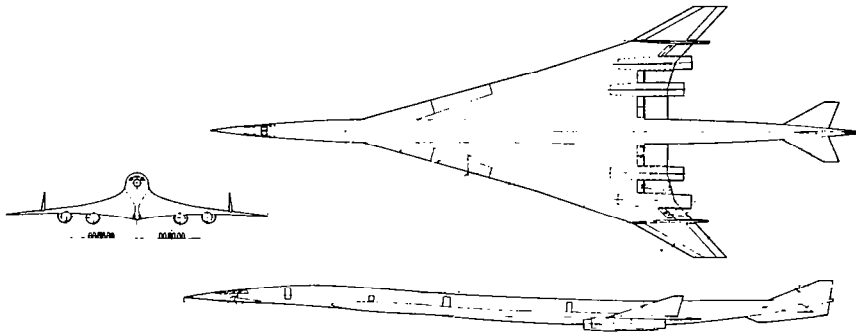
	E		ν	F_{tu}	F_{cu}	FAC	γ
	GN/m ² (ksi)			MN/m ² (ksi)			kg/m ³ (lb/in. ³)
TITANIUM ALLOY							
	110	(16.10 ³)	0.3	827 (120)	869 (126)	155 (22.5)	4429 (0.16)
GRAPHITE-POLYIMIDE, AVAILABLE IN 1986, FIBER VOLUME 60%, LOW MODULUS (LM)							
//	138	(20)	0.31	2034 (295)	1999 (290)	352 (51)	1550 (0.056)
⊥	7.8	(1.13)	0.18	115 (16.7)	113 (16.4)		
GRAPHITE-POLYIMIDE, AVAILABLE IN 1986, FIBER VOLUME 60%, HIGH MODULUS (HM)							
//	276	(40)	0.29	1020 (148)	869 (126)	177 (25.6)	1605 (0.058)
⊥	12.4	(1.8)	0.013	46 (6.7)	39.3 (5.7)		
GRAPHITE-POLYIMIDE, AVAILABLE IN 1975, FIBER VOLUME 60%, LOW MODULUS (LM)							
//	13.8	(20)	0.31	1186 (172)	1186 (172)	205 (29.8)	1550 (0.056)
⊥	15.2	(2.2)	0.18	61 (8.8)	101 (14.7)		
GRAPHITE-POLYIMIDE, AVAILABLE IN 1975, FIBER VOLUME 60%, HIGH MODULUS (HM)							
//	179	(26)	0.29	1020 (148)	869 (126)	177 (25.6)	1605 (0.058)
⊥	13.8	(2.0)	0.013	41 (5.9)	110 (16)		
GRAPHITE-POLYIMIDE, AVAILABLE IN 1975, FIBER VOLUME 60%, LOW MODULUS (LM) WITH ULTIMATE STRAIN RESTRICTED TO 0.006							
//	138	(20)	0.31	1420 (206)	1393 (202)	352 (51)	1550 (0.056)
⊥	15.2	(2.2)	0.18	115 (16.7)	113 (16.4)		
HONEYCOMB CORE							89 (0.0032)
ADHESIVE BONDING FACE SHEETS TO CORE, MASS PER AREA, kg/m ² (lb/ft ²)							0.036 (0.288)
<p>LEGEND: E YOUNG MODULUS F_{tu}, F_{cu} ULTIMATE TENSILE, COMPRESSIVE STRENGTH FAC STRESS ALLOWABLE FOR CRUISE ALL VALUES - ROOM TEMPERATURE 20 °C (68 °F) // — PARALLEL TO FIBER ⊥ — PERPENDICULAR TO FIBER</p>							

TABLE 2.- DEFINITION OF THE LOADING CASES

LOAD CASE	LOAD FACTOR [g]	MACH	ALTITUDE m, (ft)	GROSS MASS kg, (lbm)	FUEL MASS kg, (lbm)	REMARKS
CRUISE	1.0	2.7	18 288 (60 000)	313 626 (691 545)	127 212 (280 503)	AIRCRAFT BUILT TO A JIG SHAPE DEFORMS TO A SHAPE AERODYNAMICALLY MOST EFFICIENT FOR CRUISE
MANEUVER	2.5	1.2	10 668 (35 000)	340 823 (751 514)	154 410 (340 473)	SYMMETRIC PULL-UP
TAXI	-2.0	0	0	345 578 (762 000)	158 654 (349 833)	SUPPORT ON THE NOSE AND MAIN GEAR, NO AERODYNAMIC LIFT

TABLE 3.- INFLUENCE OF THE CHOICE OF DESIGN VARIABLES ON MASS AND FLUTTER SPEED

CASE	FREE VARIABLES	MASS, kg (lb)	FLUTTER SPEED DEFICIENCY ΔV , km/hr (knots)	$\frac{\Delta m}{\Delta V}$, $\frac{\text{kg}}{\text{km/hr}}$ ($\frac{\text{lb}}{\text{knots}}$)
11.1.1	$t_0, t_{\pm 45}, t_{90}$	21829 (48125)	309 (167)	27.0 (110.0)
.2	$t_0, t_{\pm 45}, t_{90}, \gamma$	21748 (47947)	335 (181)	25.1 (103.0)
.3	$t_0, t_{\pm \phi}, t_{90}, \phi$	21453 (47297)	411 (222)	21.2 (86.6)
.4	$t_0, t_{\pm \phi}, t_{90}, \gamma, \phi$	21274 (46902)	411 (222)	21.6 (88.3)
.5	$t_0, t_{\pm 45}, t_{90}, h$	20363 (44894)	309 (167)	31.7 (129.0)
.6	$t_0, t_{\pm \phi}, t_{90}, h, \phi$	19908 (43889)	456 (246)	22.5 (92.0)
.7	$t_0, t_{\pm \phi}, t_{90}, h, \phi, \gamma$	19784 (43616)	456 (246)	22.8 (93.1)



TAKE-OFF GROSS WEIGHT	346 363 kg	(762 000 lb)
OPERATION EMPTY WEIGHT	159 608 kg	(351 139 lb)
PAYLOAD	27 740 kg	(61 028 lb)
LENGTH	96 m	(315 ft)
SPAN	42 m	(138 ft)
CRUISE SPEED	M = 2.7	

Figure 1.- Basic characteristics of the arrow wing supersonic cruise vehicle.

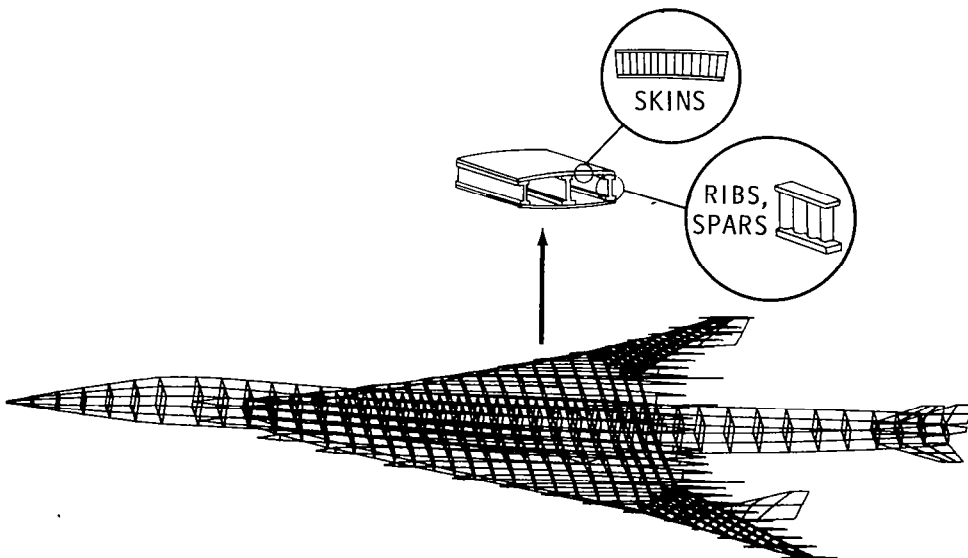


Figure 2.- Finite-element model with details of the wing construction.

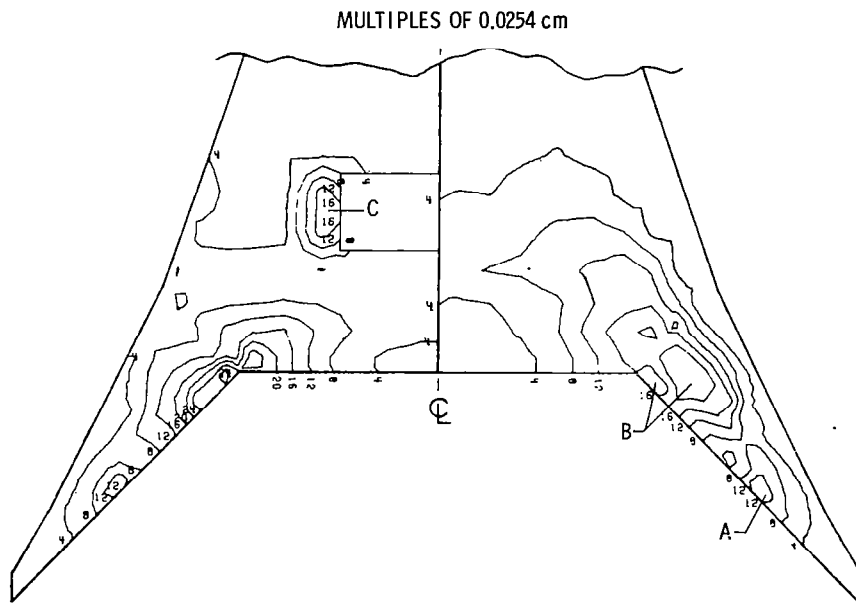


Figure 3.- Strength design thickness distribution.

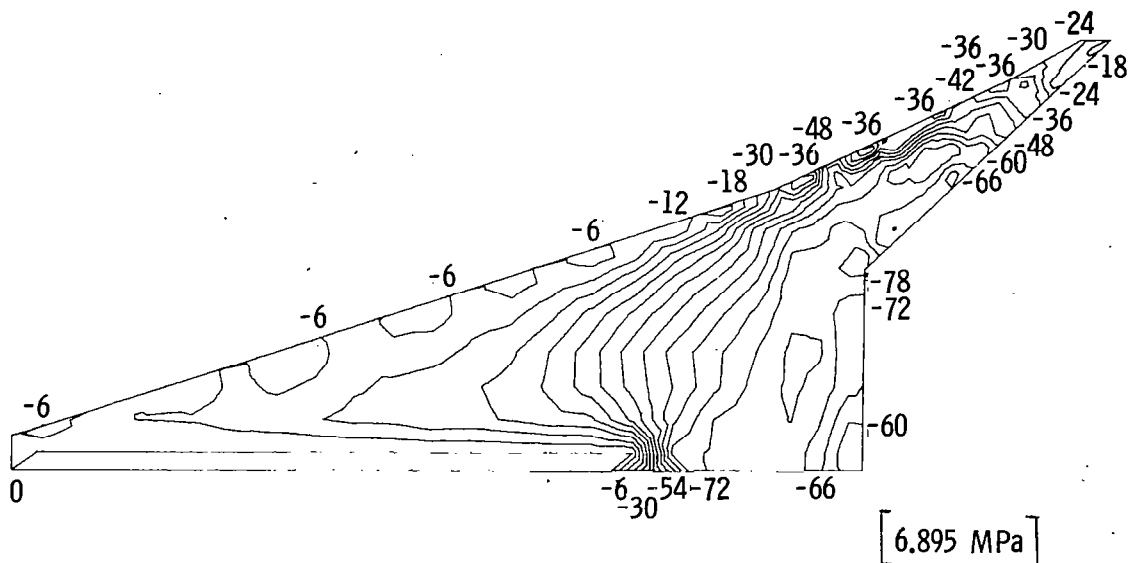


Figure 4.- Minimum (maximum compression) principal stress distribution in the upper cover for the maneuver condition.

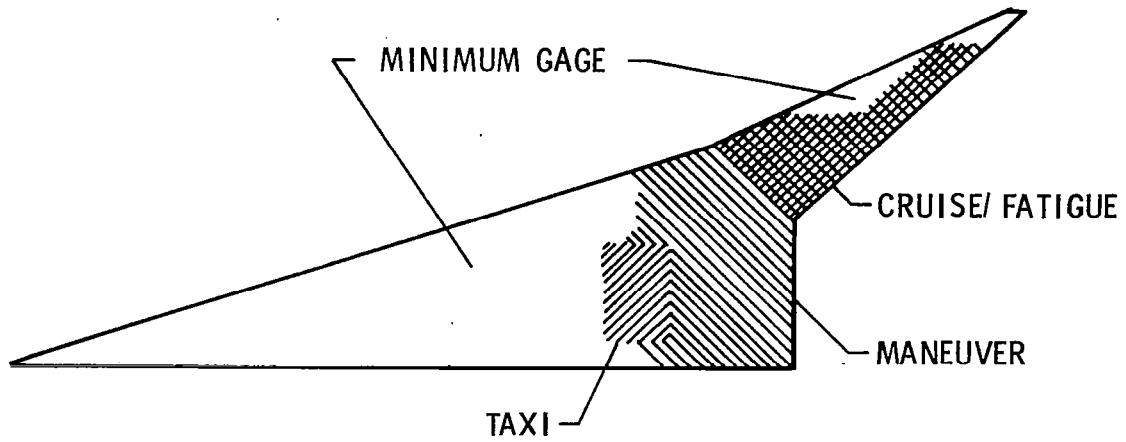


Figure 5.- Critical loading cases for defined wing areas.

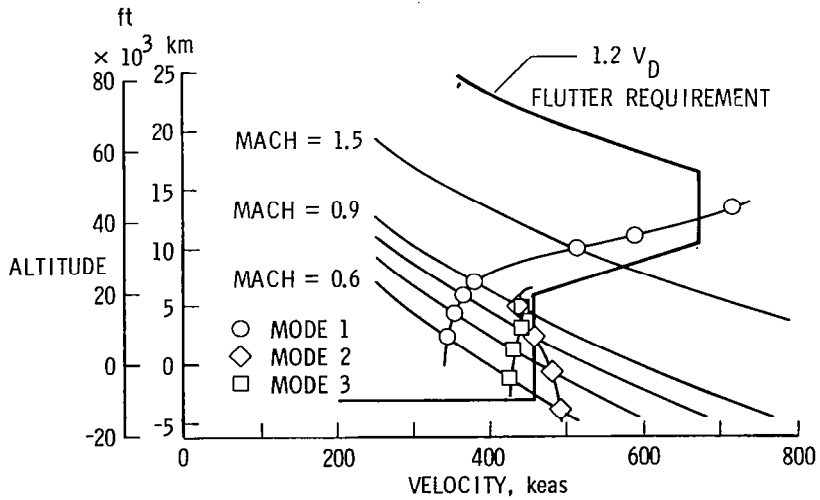


Figure 6.- Flutter boundaries for the strength sized baseline (9.1, E23) configuration, and the required flutter-free envelope.

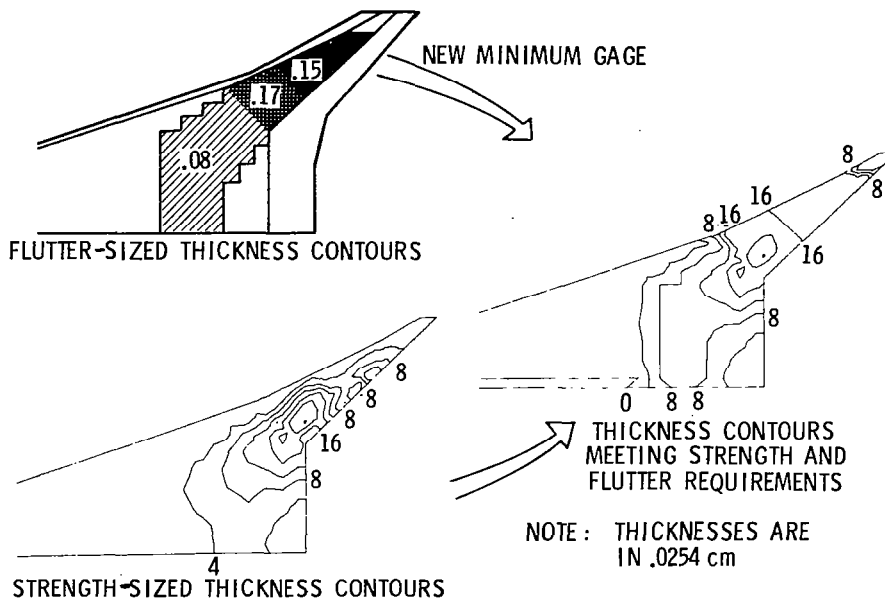


Figure 7.- Combining the strength designed wing cover thicknesses with those required for the flutter fix by means of the "new minimum gage" technique.

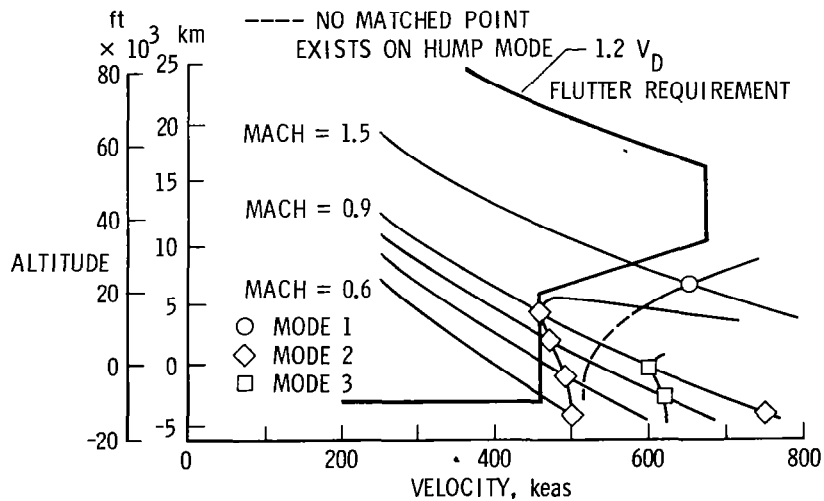


Figure 8.- Flutter boundaries for the flutter-fixed baseline (9.1, E23) configuration moved beyond the required envelope.

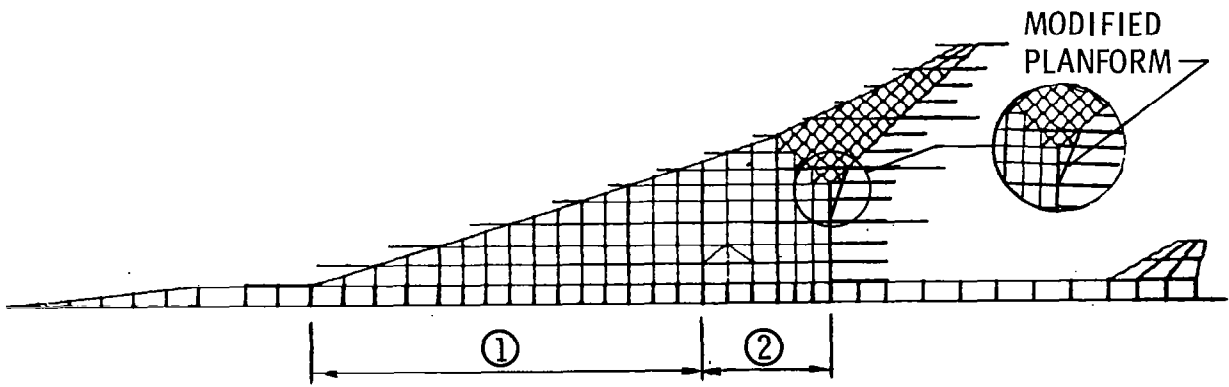


Figure 9.- Modified carry-through and "double crank" (inset) configuration.

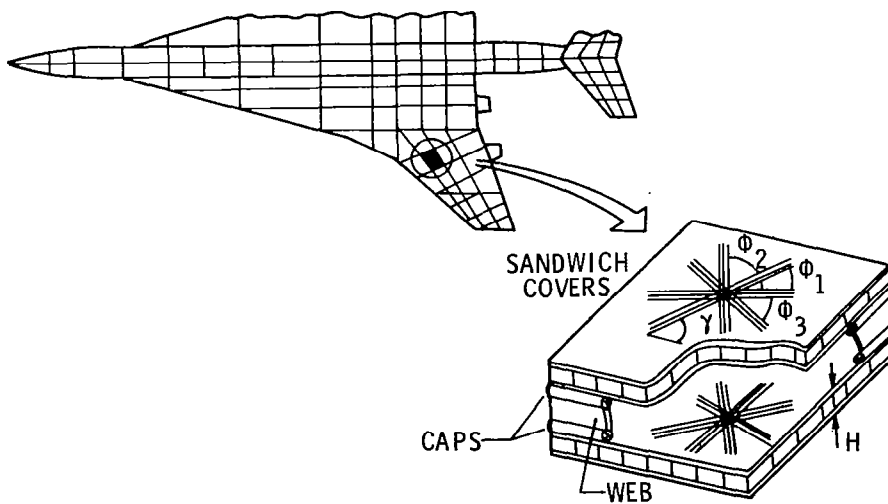


Figure 10.- Composite sandwich wing covers.

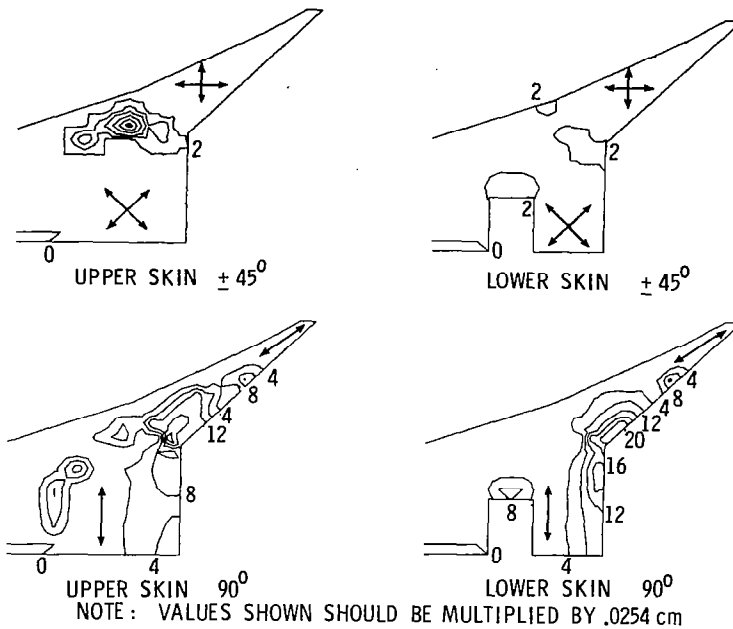


Figure 11.- Strength design thickness distributions of the composite material layers.

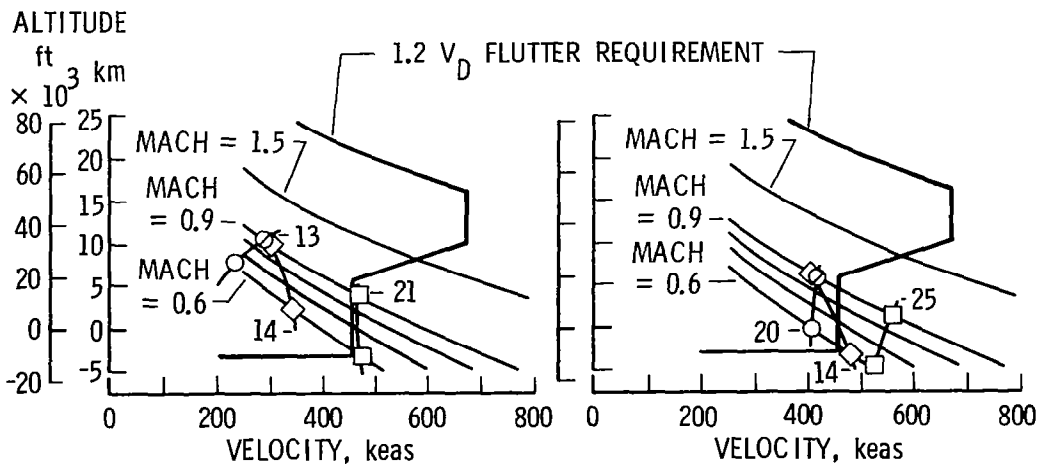


Figure 12.- Flutter deficiency of the strength sized hybrid configuration (variant 11.1.1) for low Young's modulus material (left) and high Young's modulus material (right).

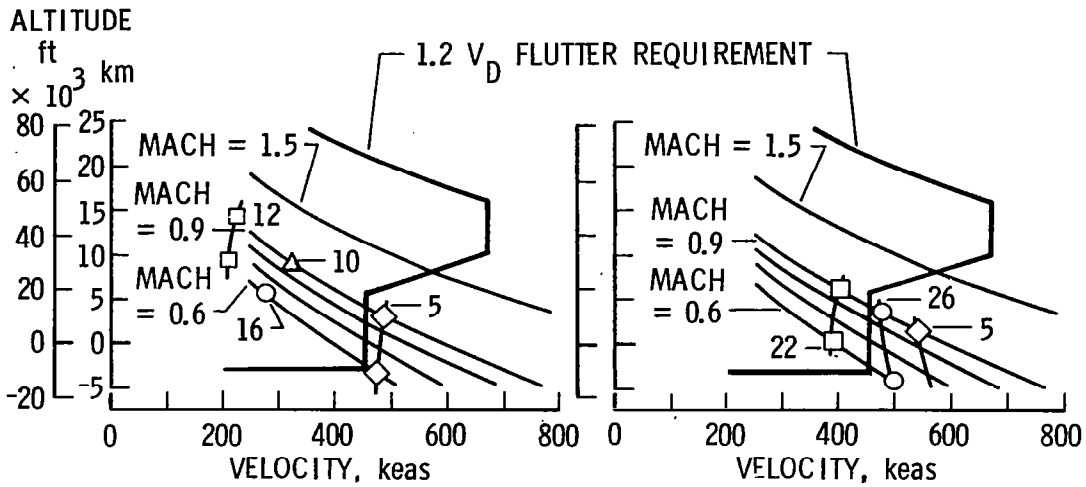


Figure 13.- Flutter deficiency of the strength sized pure composite configuration (11.2) for low Young's modulus material (left), and high Young's modulus material (right).

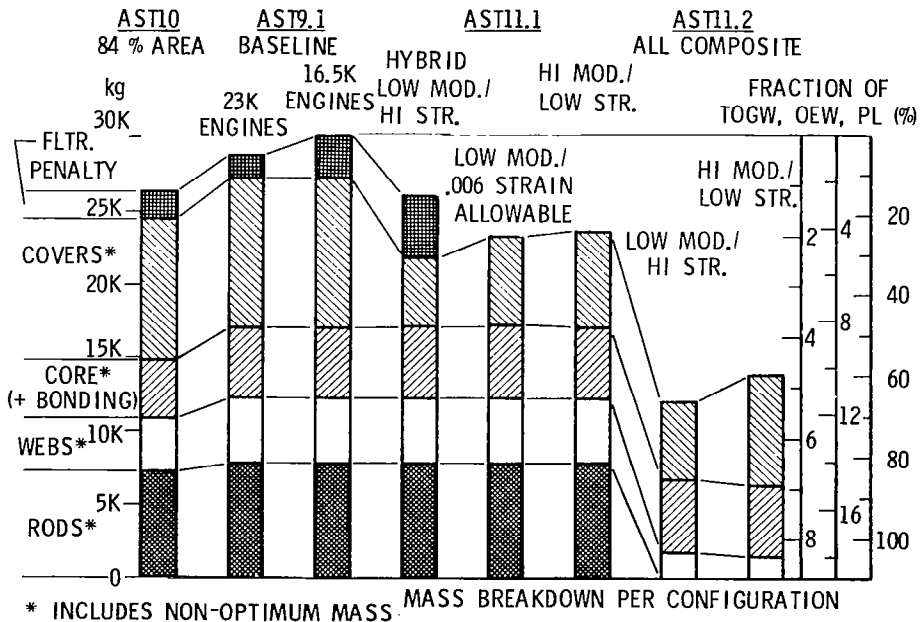


Figure 14.- Comparison of the total structural masses and their components.

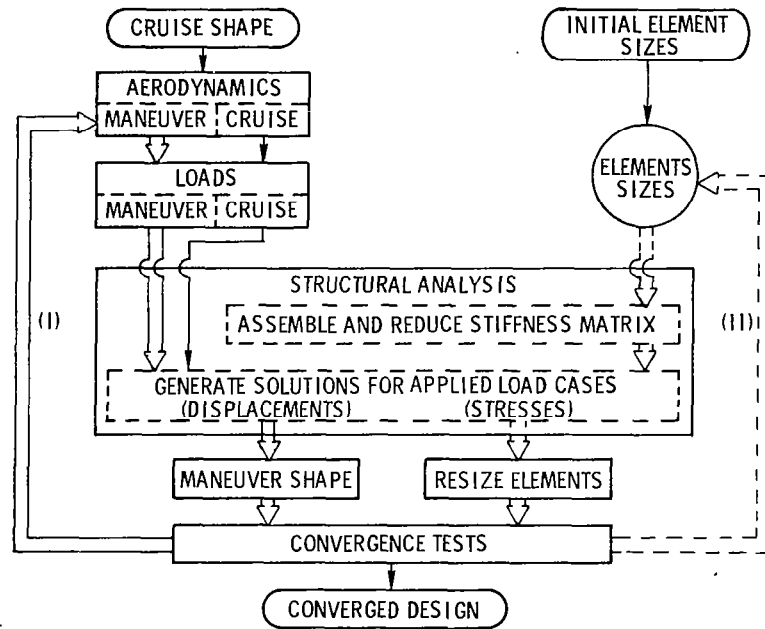


Figure 15.- Iterative procedures for aeroelastic loads computation (loop I) and wing cover resizing (loop II).

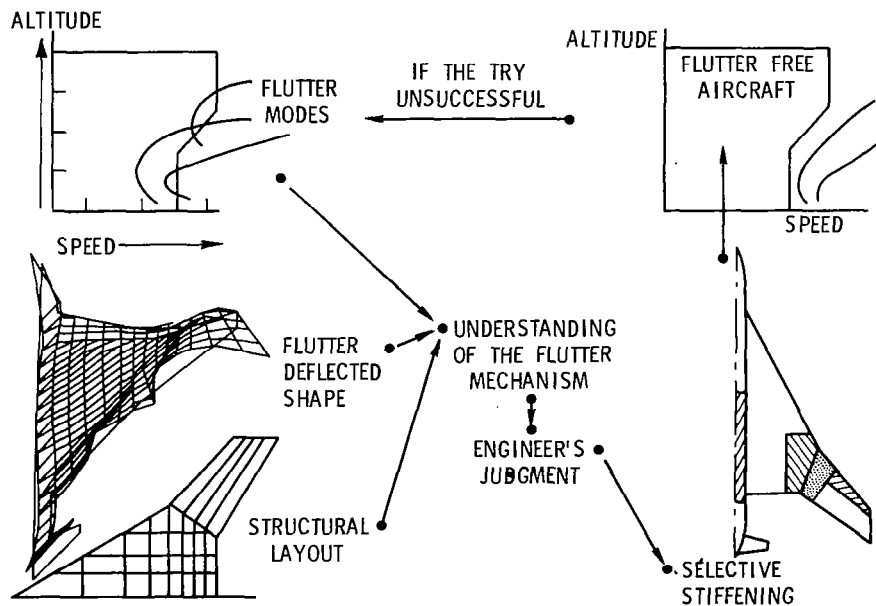


Figure 16.- Trial-and-error flutter fix procedure.

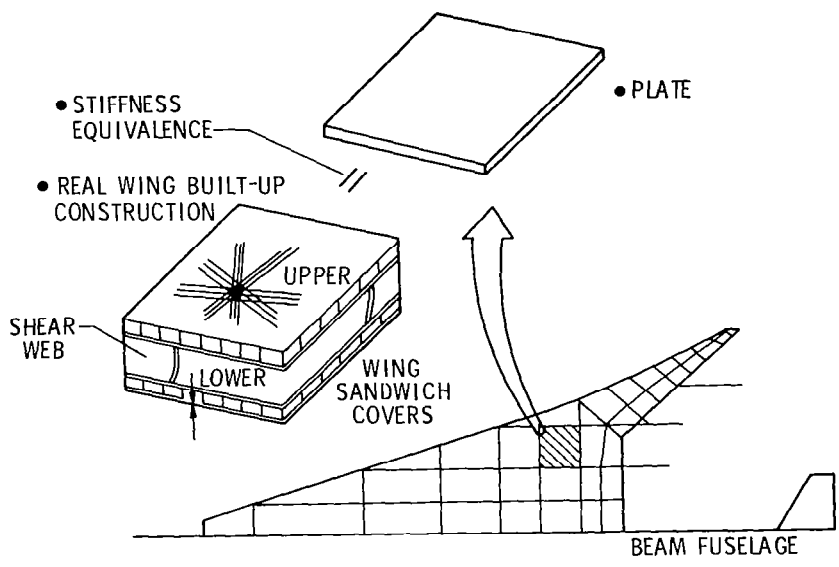


Figure 17.- "Small" model equivalent to "large" model with respect to mass and bending stiffness.